SUPPLEMENTARY INFORMATION ACCOMPANIES THIS MANUSCRIPT

SUPPLEMENTAL METHODS

BTK mutation analysis in patients

To check BTK mutations, a cohort of 755 pre-treatment lymphoma specimens [follicular lymphoma (FL, n=199), mantle cell lymphoma (MCL, n=197), diffuse large B-cell lymphoma (DLBCL, n=148), Burkitt's lymphoma (BL, n=107), chronic lymphocytic leukemia / small lymphocytic lymphoma (CLL/SLL, n=45), splenic/nodal marginal zone lymphoma (MZL, n=24), high-grade B-cell lymphoma NOS (HGBL-NOS, n=21) or double-hit lymphoma (DHL, n=14)] were interrogated by targeted sequencing, as previously described (1). In brief, 500ng-1µg of tumor DNA was sheared by sonication using a Covaris S2 instrument, and end repaired, A-tailed and ligated with Illumina TruSeq adaptors (Bio-O Scientific) using Kapa HyperPrep Kits (Kapa Biosystems). Adapter ligated products were enriched using 6 cycles of PCR, and 12-plexed for hybrid capture using a custom hybrid capture reagent (Nimblegen) that included all coding exons for *BTK*. Each pool was sequenced with 100bp paired end reads on a single lane of a HiSeq 2500 Instrument in high output mode at the Hudson Alpha Institute for Biotechnology. Raw sequencing reads were aligned to the human genome (hg19) using a BWA-Mem(2), realigned around InDels using GATK(3), sorted and deduplicated using Piccard tools, and variants were called according to a consensus between VarScan2(4) and GATK Unified Genotyper (3). This approach has been validated to have a specificity of 92.9% and a sensitivity of 86.7%(5). Average on-target rate for this dataset was 88% and average depth of coverage 599X (min = 101X, max = 1785X). In addition, BTK mutations were identified from our targeted genomic database of Lymphoma Cohort that includes 820 samples from

795 patients. Targeted mutational sequencing was performed with either Foundation One Heme or MSK-IMPACT assay. Patients on the Memorial Sloan-Kettering Cancer Center (MSKCC) lymphoma service were referred for targeted mutational sequencing since Jan 2013. Clinical data were collected based on clinician assessment. This study was conducted under the context of a retrospective waiver under institutional review board approval to determine clinical utility of targeted genomic sequencing. Informed consent for biospecimen banking and sequencing was obtained from all participating patients. We also analyzed BTK mutations in published genomic studies (6-9). BTK mutation analysis was performed using cbioportal (http://www.cbioportal.org) (10, 11).

Reference

1. Garcia-Ramirez I, Tadros S, Gonzalez-Herrero I, Martin-Lorenzo A, Rodriguez-Hernandez G, Moore D, Ruiz-Roca L, Blanco O, Alonso-Lopez D, De Las Rivas J, et al. Crebbp loss cooperates with Bcl2 over-expression to promote lymphoma in mice. *Blood.* 2017;129(19):2645-56.
2. Li H. Aligning sequence reads, clone sequences and assembly contigs with BWA-MEM. *arXiv.* 2013;1303.3997(
3. McKenna A, Hanna M, Banks E, Sivachenko A, Cibulskis K, Kernytsky A, Garimella K, Altshuler D, Gabriel S, Daly M, et al. The Genome Analysis Toolkit: a MapReduce framework for analyzing next-generation DNA sequencing data. *Genome research.* 2010;20(9):1297-303.
4. Koboldt DC, Zhang Q, Larson DE, Shen D, McLellan MD, Lin L, Miller CA, Mardis ER, Ding L, and Wilson RK. VarScan 2: somatic mutation and copy number alteration discovery in cancer by exome sequencing. *Genome research.* 2012;22(3):568-76.

5. Green MR, Kihira S, Liu CL, Nair RV, Salari R, Gentles AJ, Irish J, Stehr H, Vicente-Duenas C, Romero-Camarero I, et al. Mutations in early follicular lymphoma progenitors are associated with suppressed antigen presentation. *Proceedings of the National Academy of Sciences of the United States of America.* 2015;112(10):E1116-25.
6. Reddy A, Zhang J, Davis NS, Moffitt AB, Love CL, Waldrop A, Leppa S, Pasanen A, Meriranta L, Karjalainen-Lindsberg ML, et al. Genetic and Functional Drivers of Diffuse Large B Cell Lymphoma. *Cell.* 2017;171(2):481-94 e15.
7. Krysiak K, Gomez F, White BS, Matlock M, Miller CA, Trani L, Fronick CC, Fulton RS, Kreisel F, Cashen AF, et al. Recurrent somatic mutations affecting B-cell receptor signaling pathway genes in follicular lymphoma. *Blood.* 2017;129(4):473-83.
8. Lohr JG, Stojanov P, Lawrence MS, Auclair D, Chapuy B, Sougnez C, Cruz-Gordillo P, Knoechel B, Asmann YW, Slager SL, et al. Discovery and prioritization of somatic mutations in diffuse large B-cell lymphoma (DLBCL) by whole-exome sequencing. *Proc Natl Acad Sci U S A.* 2012;109(10):3879-84.
9. Morin RD, Mungall K, Pleasance E, Mungall AJ, Goya R, Huff RD, Scott DW, Ding J, Roth A, Chiu R, et al. Mutational and structural analysis of diffuse large B-cell lymphoma using whole-genome sequencing. *Blood.* 2013;122(7):1256-65.
10. Gao J, Aksoy BA, Dogrusoz U, Dresdner G, Gross B, Sumer SO, Sun Y, Jacobsen A, Sinha R, Larsson E, et al. Integrative analysis of complex cancer genomics and clinical profiles using the cBioPortal. *Sci Signal.* 2013;6(269):pl1.
11. Cerami E, Gao J, Dogrusoz U, Gross BE, Sumer SO, Aksoy BA, Jacobsen A, Byrne CJ, Heuer ML, Larsson E, et al. The cBio cancer genomics portal: an open platform for exploring multidimensional cancer genomics data. *Cancer Discov.* 2012;2(5):401-4.

SUPPLEMENTAL FIGURE LEGENDS

Supplemental Figure 1. BTK mutations affecting covalent BTK inhibitor. (A) BTK mutations reported in publications and in TCGA Lymphoid Neoplasm Diffuse Large B-cell Lymphoma project. Detailed amino acid change and source of original data are indicted in Supplemental Table 2. (B) Diagram of the BTK mutagenesis screen in BCL1 lymphoma cells. (C) FACS analysis shows enrichment of GFP (co-expressed with mutant BTK) after ibrutinib treatment. (D) BTK sequences representing 350 enriched clones; frequencies for common BTK mutations in the pie chart. (D) Immunoblot analysis of BTK Y223 auto-phosphorylation in HEK293T cells that express the indicated BTK alleles and lack endogenous BTK, treated with ibrutinib. Total BTK was used as a control and quantification was done with ImageJ.

Supplemental Figure 2. Quality control of two BTK mutagenesis CDS libraries. (A) and (B) Deep sequencing analysis of two separate BTK mutagenesis libraries generated independently from XL-1 red E. coli cells. X-axis indicates the distribution of occurring frequency of BTK mutation and Y-axis demonstrates the density of each occurring mutation frequency. Left panel shows the overall nucleotide variance and right panel shows only the nonsense and missense nucleotide variance in both (A) and (B).

Supplemental Figure 3. Validation of ibrutinib screen results with ibrutinib and RN486. (A-B) Cell proliferation assay of BCL1 lymphoma cells expressing the BTK wild type or mutant alleles and treated with ibrutinib (A) or RN486 (B) at indicated dose range for 72 hours. Viable cells were determined by CellTiter-Glo and normalized to DMSO

treatment. (C-D) Analogous results from TMD8 cells treated with Ibrutinib (C) or RN486 (D).

Supplemental Figure 4. Validation of screen results with additional covalent and non-covalent inhibitors. (A-C) Cell proliferation assay of TMD8 lymphoma cells expressing the indicated BTK wild type or mutant alleles were treated with covalent inhibitor Acalabrutinib (A) or non-covalent inhibitor GDC-0853 (B) or SNS-062 (C) at indicated dose range for 72 hours. Viable cells were determined by CellTiter-Glo and normalized to DMSO treatment.

Supplemental Figure 5. Effect of BTK mutant alleles on BTK auto-phosphorylation and downstream signaling. (A) BTK (Y223) auto-phosphorylation in HEK293T cells measured by FACS, excerpt from Figure 3A focusing on differences between different C481 mutations. Data are represented as mean ± SD from 2 independent experiments. * $p < 0.05$ vs. WT_BTK determined by Student's. t test. (B) BTK_E41K is a reported gain of function mutation and causes increased auto-phosphorylation (Y223) compared to WT_BTK in HEK293T cells. Data are represented as mean ± SD from 2 independent experiments. * $p < 0.05$ vs. WT_BTK determined by Student's. t test. (C) Immunoblot on TMD8 lysates expressing indicated wild type or mutant BTK alleles probed for BTK auto-phosphorylation and downstream signaling. (D) Immunoblot on TMD8 lysates expressing indicated wild type or mutant BTK alleles probed for BTK auto-phosphorylation and downstream signaling following anti-IgM stimulation. Total protein was used as a control for corresponding phosphor protein and quantification was done with ImageJ in both C and D.

Supplemental Figure 6. Residue-level contacts in molecular dynamics trajectories of BTK mutant alleles. (A-B) The frequency of contacts between all pairs of residues was quantified in wild type BTK (WT_ BTK) (A) and the BTK mutants T474M, E513G and T474M+E513G (B). Changes in residue-level contact patterns associated with mutations were quantified by subtracting the contact frequencies in the wild type BTK from that in each mutant (C). Each point in the 2D matrix corresponds to a pair of residues labeled along the X- and Y-axes respectively, with values ranging from 0 (no contact) to 1 (contact all the time). A residue pair scoring close to 1 or -1 in the matrix has differential contact in the mutant compared to wild type. (D) The top twenty peaks in the contact map (top-scoring pairs of residues) are mapped onto the specific residues in the protein model. These residues are highlighted in stick representation, and the residue being mutated in all-atom CPK representation. Strong signals emerge in the double mutant connecting the mutations to residues implicated in activation, viz. D579 and H519.

Supplemental Table 1: BTK mutations identified in ibrutinib naïve lymphoma specimens in this study

Supplemental Table 2: Published BTK mutations in ibrutinib naïve lymphomas

Supplemental Table 3: Deep sequencing of BTK library 1

Supplemental Table 4: Deep sequencing of BTK library 2

Supplemental Table 5: PCR primers

Suppl. Figure 1

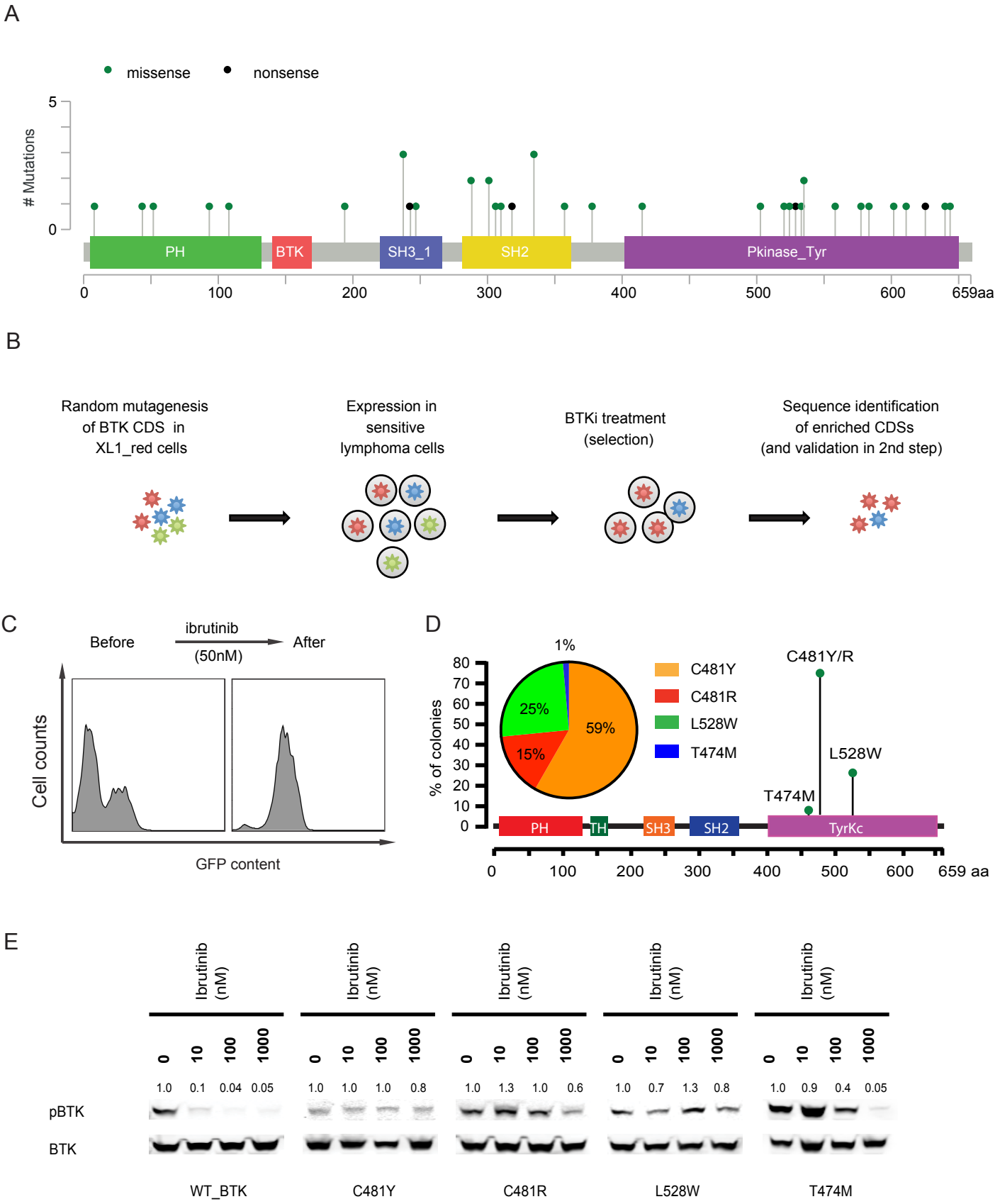

A

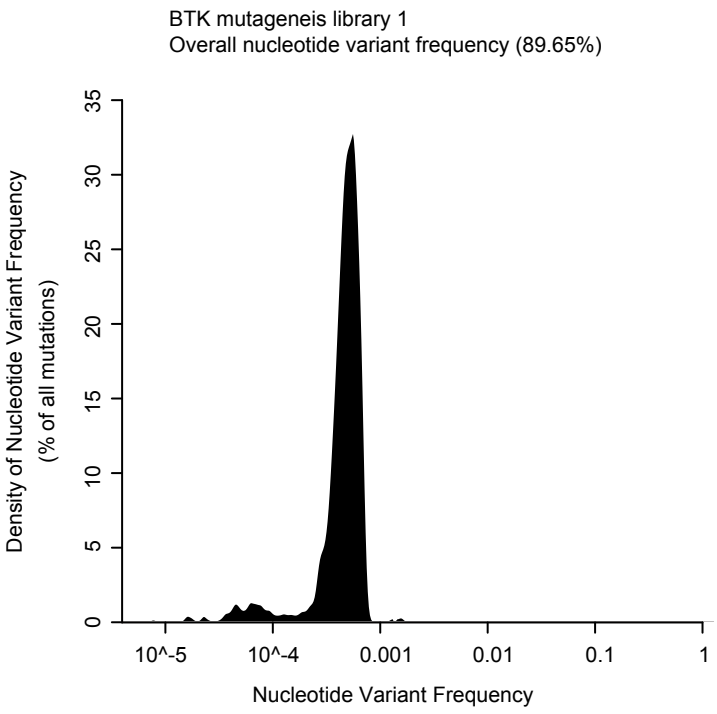
BTK mutageneis library 1
Overall nucleotide variant frequency (89.65%)
Density of Nucleotide Variant Frequency
(% of all mutations)
0
5
10
15
20
25
30
35
10^-5
10^-4
0.001
0.01
0.1
1
Nucleotide Variant Frequency

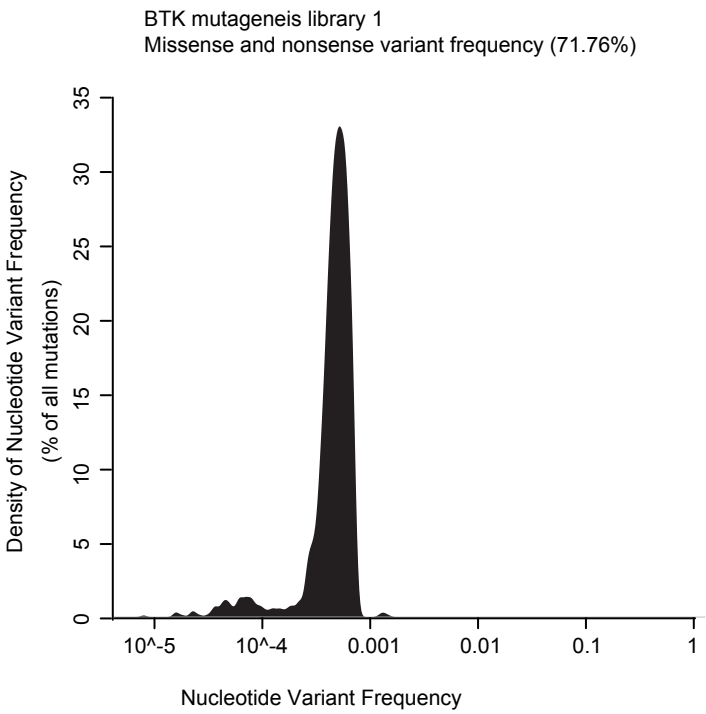
BTK mutageneis library 1
Missense and nonsense variant frequency (71.76%)
Density of Nucleotide Variant Frequency
(% of all mutations)
0
5
10
15
20
25
30
35
10^-5
10^-4
0.001
0.01
0.1
1
Nucleotide Variant Frequency

B

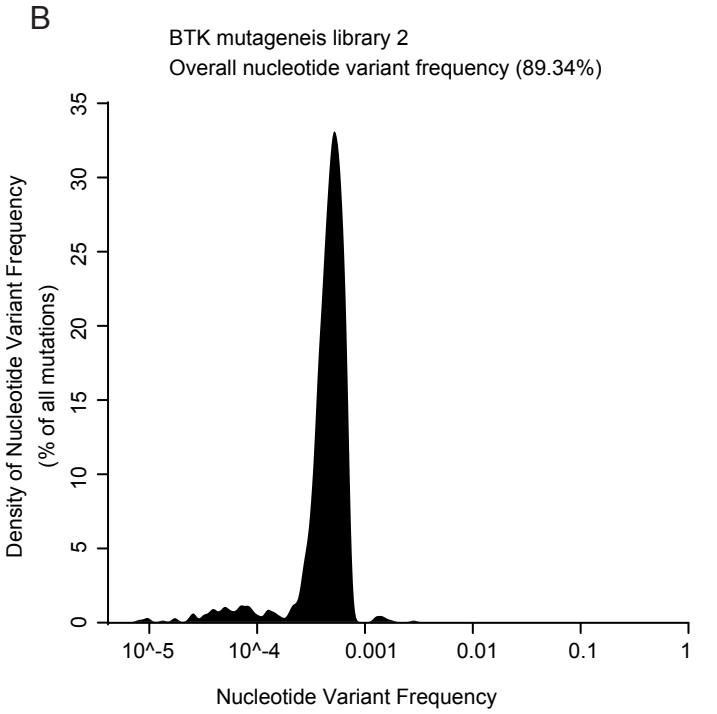
BTK mutageneis library 2
Overall nucleotide variant frequency (89.34%)
Density of Nucleotide Variant Frequency
(% of all mutations)
0
5
10
15
20
25
30
35
10^-5
10^-4
0.001
0.01
0.1
1
Nucleotide Variant Frequency

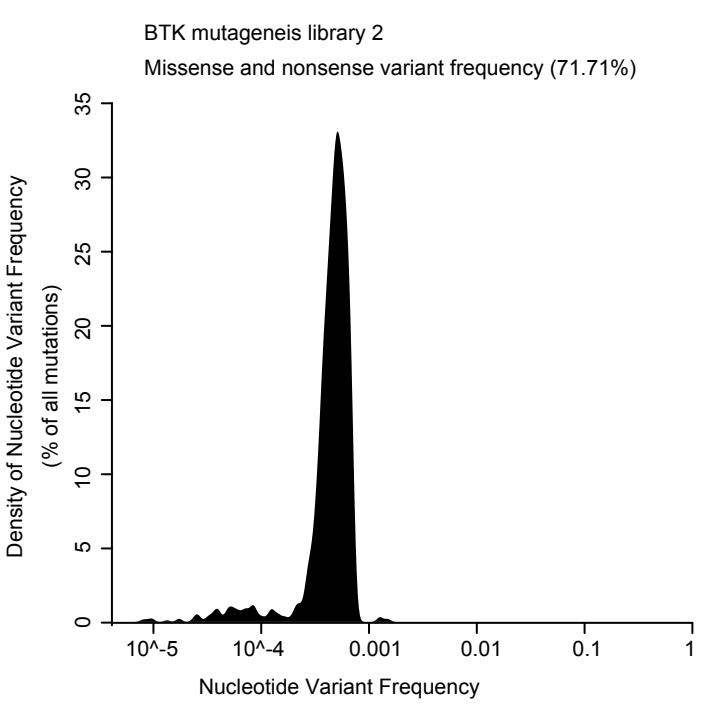
BTK mutageneis library 2
Missense and nonsense variant frequency (71.71%)
Density of Nucleotide Variant Frequency
(% of all mutations)
0
5
10
15
20
25
30
35
10^-5
10^-4
0.001
0.01
0.1
1
Nucleotide Variant Frequency

Suppl. Figure 3

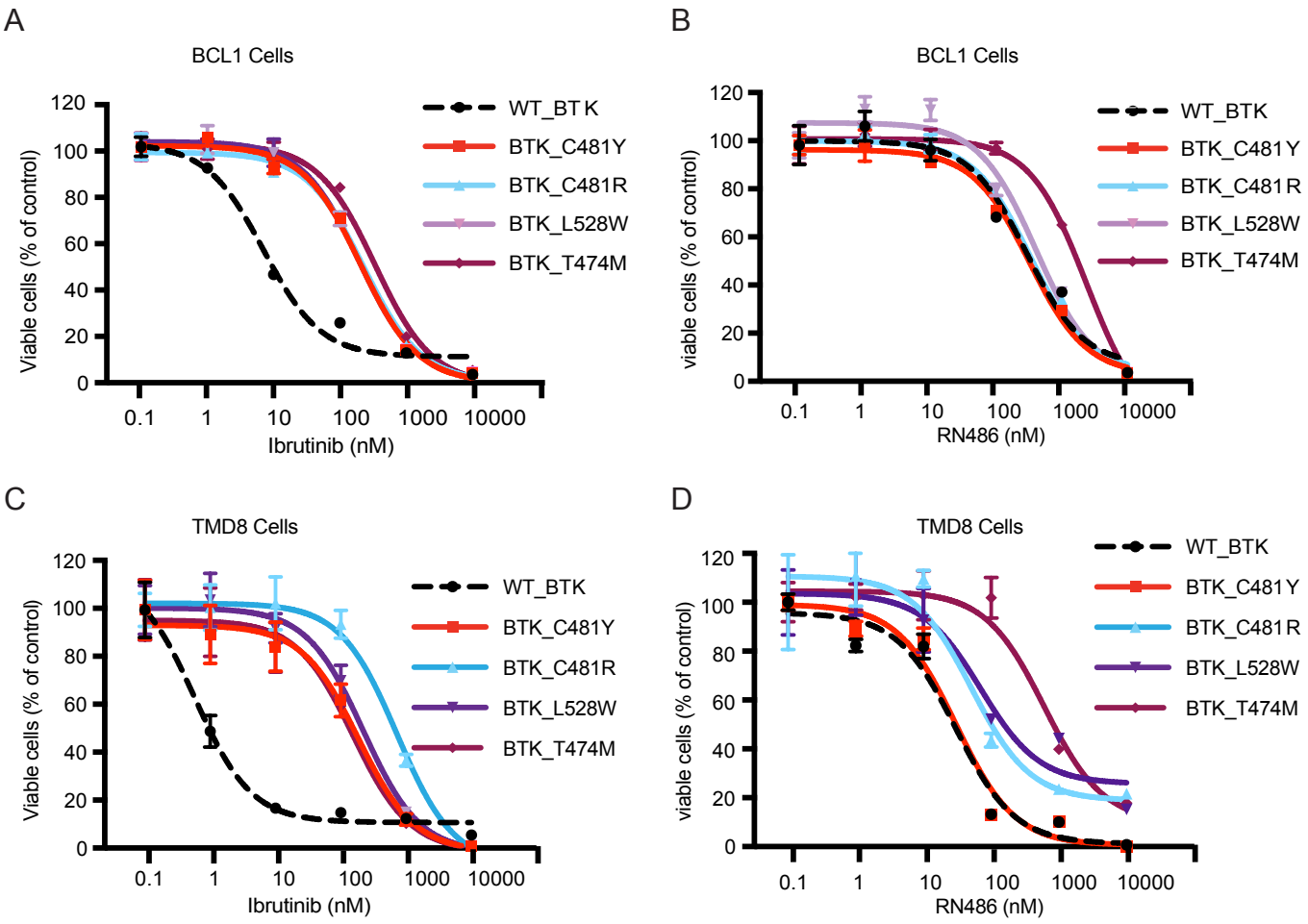

A

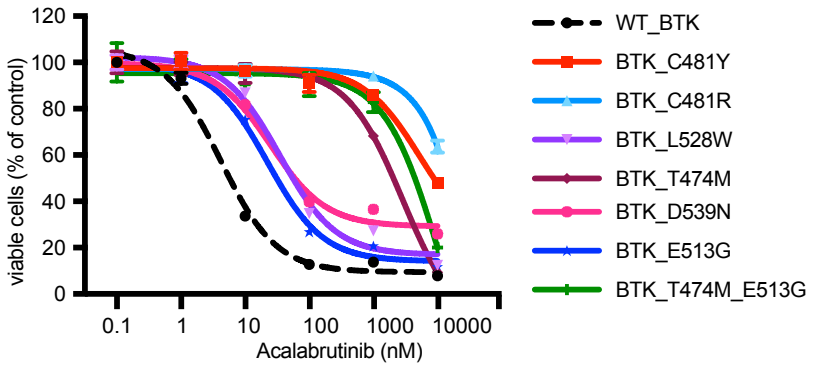
viable cells (% of control)
120
100
80
60
40
20
0
0.1
1
10
100
1000
10000
Acalabrutinib (nM)
WT_BTK
BTK_C481Y
BTK_C481R
BTK_L528W
BTK_T474M
BTK_D539N
BTK_E513G
BTK_T474M_E513G

B

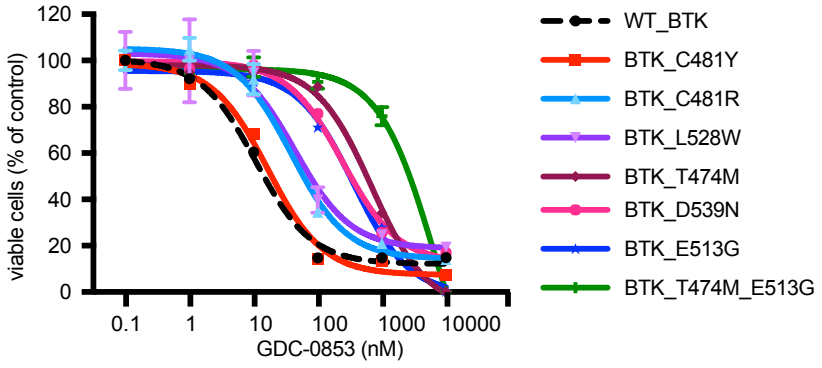
viable cells (% of control)
120
100
80
60
40
20
0
0.1
1
10
100
1000
10000
GDC-0853 (nM)
WT_BTK
BTK_C481Y
BTK_C481R
BTK_L528W
BTK_T474M
BTK_D539N
BTK_E513G
BTK_T474M_E513G

C

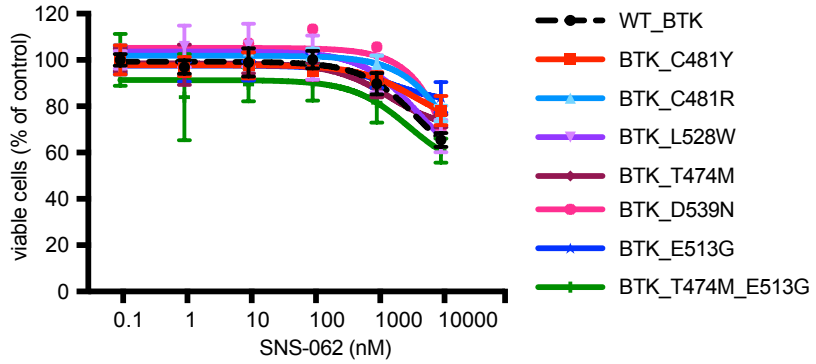
viable cells (% of control)
120
100
80
60
40
20
0
0.1
1
10
100
1000
10000
SNS-062 (nM)
WT_BTK
BTK_C481Y
BTK_C481R
BTK_L528W
BTK_T474M
BTK_D539N
BTK_E513G
BTK_T474M_E513G

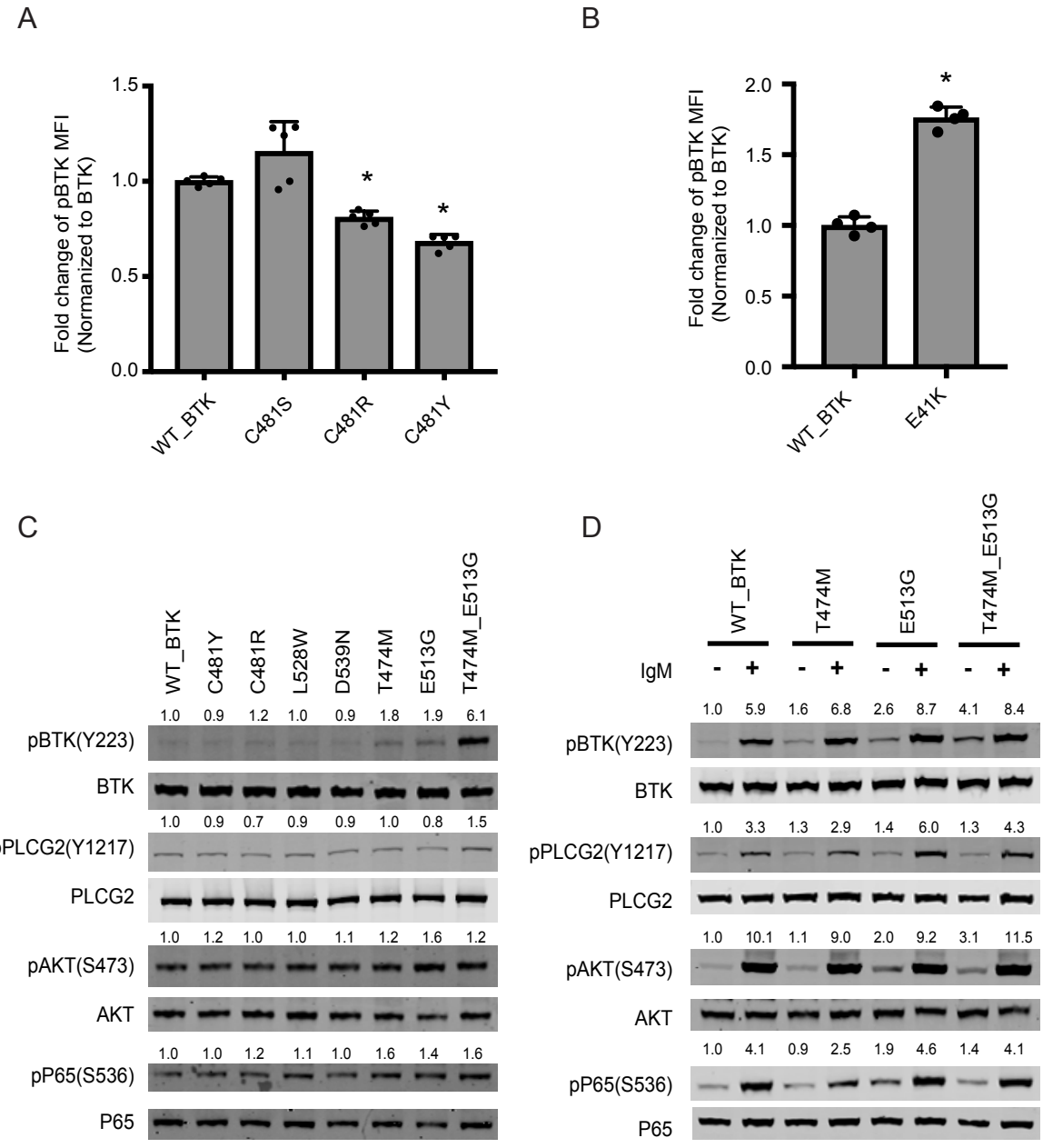
A
Fold change of pBTK MFI (Normanized to BTK)
1.5
1.0
0.5
0.0
*
*
WT_BTK
C481S
C481R
C481Y
B
Fold change of pBTK MFI (Normanized to BTK)
2.0
1.5
1.0
0.5
0.0
*
WT_BTK
E41K
C
WT_BTK
C481Y
C481R
L528W
D539N
T474M
E513G
T474M_E513G
pBTK(Y223)
1.0 0.9 1.2 1.0 0.9 1.8 1.9 6.1
BTK
1.0 0.9 0.7 0.9 0.9 1.0 0.8 1.5
pPLCG2(Y1217)
PLCG2
1.0 1.2 1.0 1.0 1.1 1.2 1.6 1.2
pAKT(S473)
AKT
1.0 1.0 1.2 1.1 1.0 1.6 1.4 1.6
pP65(S536)
P65
D
WT_BTK
T474M
E513G
T474M_E513G
IgM
- + - + - + - +
pBTK(Y223)
1.0 5.9 1.6 6.8 2.6 8.7 4.1 8.4
BTK
pPLCG2(Y1217)
1.0 3.3 1.3 2.9 1.4 6.0 1.3 4.3
PLCG2
pAKT(S473)
1.0 10.1 1.1 9.0 2.0 9.2 3.1 11.5
AKT
pP65(S536)
1.0 4.1 0.9 2.5 1.9 4.6 1.4 4.1
P65

A

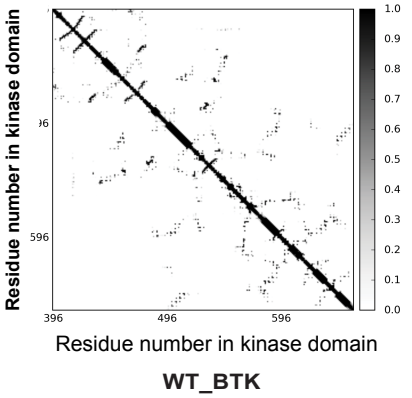
Residue number in kinase domain
Residue number in kinase domain
WT_BTK

B

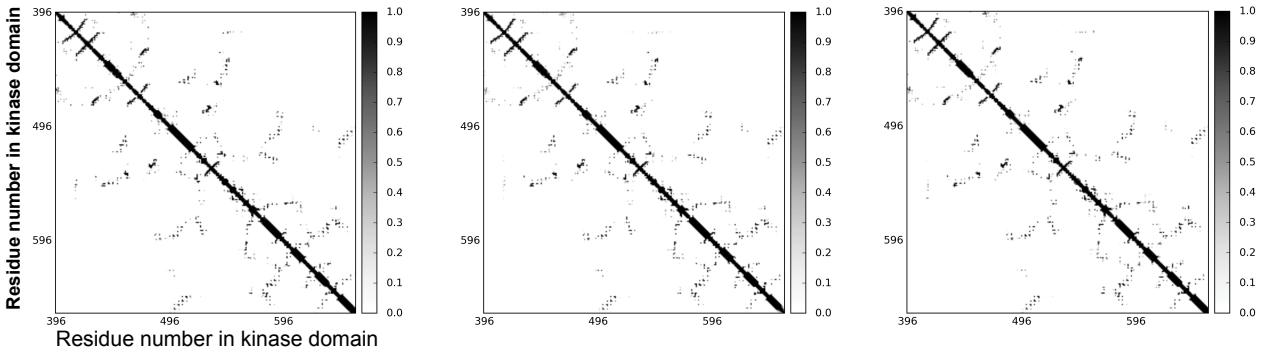
Residue number in kinase domain
Residue number in kinase domain

C

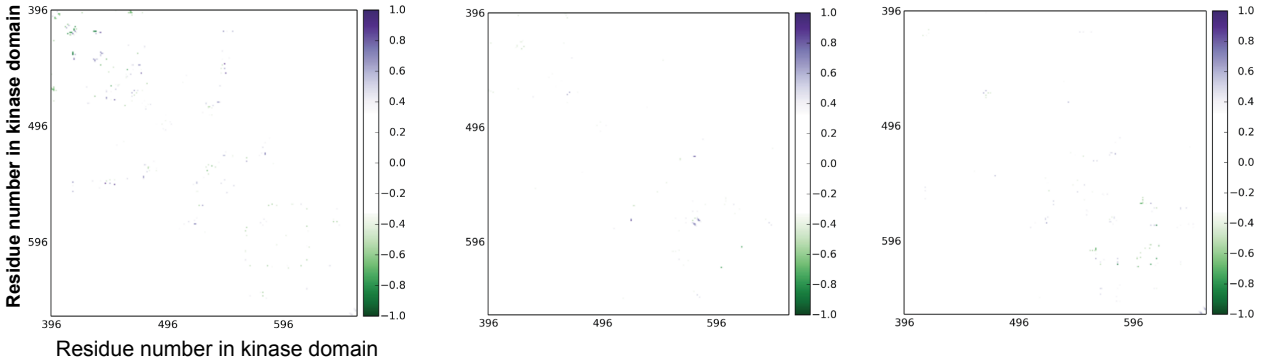
Residue number in kinase domain
Residue number in kinase domain

D

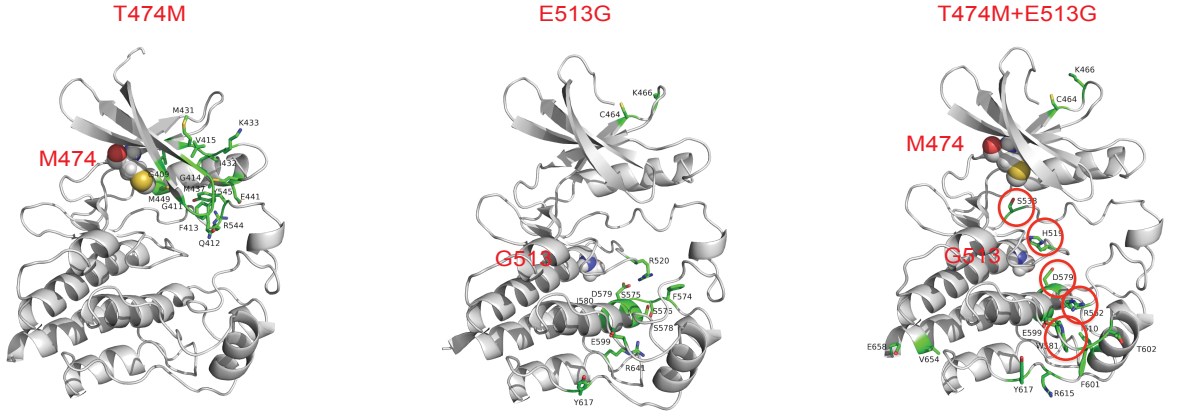
T474M
E513G
T474M+E513G
M474
G513
M474
G513